Numerical computation of noise radiation from breaking systems for squeal noise prediction

Denis Duhamel

11th World Congress on Computational Mechanics (WCCM XI)
5th European Conference on Computational Mechanics (ECCM V)
6th European Conference on Computational Fluid Dynamics (ECFD VI)
E. Oñate, J. Oliver and A. Huerta (Eds)

NUMERICAL COMPUTATION OF NOISE RADIATION FROM BREAKING SYSTEMS FOR SQUEAL NOISE PREDICTION

D. DUHAMEL*

* Université Paris-Est, Laboratoire Navier, ENPC/IFSTTAR/CNRS
6 et 8 Avenue Blaise Pascal, Cité Descartes, Champs sur Marne,
77455 Marne la Vallée, cedex 2, France
Tel: + 33 1 64 15 37 28, Fax: + 33 1 64 15 37 41
email : denis.duhamel@enpc.fr

Key words: Noise, Radiation, Squeal, Brake, High frequency

Abstract. Many trains have braking systems made of discs and pads which can generate very high noise levels. During the braking, instabilities can be generated in the contact zone between the pads and the disc, leading to high vibrations and high levels of noise radiations for frequencies typically between 1kHz and 15kHz. Numerical computations of noise radiation at these high frequencies for systems having the size of usual train braking systems and their geometrical complexities are difficult with classical methods and thus require special attention. In this paper, different strategies based on the boundary element methods and approximate methods are used for computing the sound radiation from the knowledge of the surface velocity. Contributions of parts of the system such as the disc, the pads and the caliper to the global sound levels are identified. Analysis of the system radiation in terms of spectra and directivities are also presented.

1 SQUEAL NOISE

1.1 Introduction

Recent railways vehicles are equipped with disc brakes. For some systems, braking may be accompanied by intense squeal noise. Detailed studies show that the braking system is responsible for the overall noise and brake pads play an important role in the squeal noise generation. The squeal noise generation seems highly linked to friction conditions between the disc and the pads. Instabilities are created in the contact zone between the pads and the disc leading to high vibrations and then to high levels of noise radiation. The global numerical simulation of vibrations and noise radiation of these systems are necessary to understand their physical behavior in a first step and to build quieter systems as a final aim. Analysis of these systems shows that noise spectra are generally made of discrete

frequencies corresponding to unstable vibration modes. These instabilities are responsible for the high levels of vibration. The unstable modes are usually located in the middle and high frequency ranges, and can generate sound as loud as 100dBA. Prediction methods are needed to clearly explain this phenomenon and to compute the noise levels from the knowledge of geometrical and mechanical properties of these systems, see [1, 9, 4, 6]. Finite element methods are often used for this purpose. This allows to predict several types of instabilities and gives the vibrations of the structure by a time domain analysis. This approach is suited for braking at constant force which leads to stationary noise or noise levels with low variation with time which is the current and interesting situation. Then, from a Fourier analysis, the vibrations at different frequencies of the braking system can be computed. Finally the sound radiation has to be estimated to find the acoustic power which is radiated and the sound levels at different points in the exterior domain. This paper focuses on this sound radiation. The main feature of this problem is that the systems vibrate at high frequencies, typically between 1kHz and 15kHz. It is therefore necessary to use specific methods adapted to the calculation of radiation for this range of frequencies. According to the frequency, usual boundary element methods, fast multipole boundary elements methods or high frequency approximations are used and compared for these problems. Sound powers and noise levels are computed for different parts of the braking system. Then conclusions are presented.

1.2 Acoustic problem

To compute the sound pressure p in air, one has to solve the following Helmholtz equation:

$$\begin{aligned} \Delta p(\mathbf{x}) + k^2 p(\mathbf{x}) &= 0 \quad \forall \mathbf{x} \in \Omega \\ \frac{\partial p}{\partial n}(\mathbf{x}) &= i\rho\omega v_n \quad \forall \mathbf{x} \in S \end{aligned} \tag{1}$$

where $k = \frac{\omega}{c}$ is the wavenumber, ω the circular frequency, c the sound velocity in air, v_n the normal velocity at the exterior surface of the braking system, Ω the air domain and S the exterior boundary between air and the braking system.

The solution of equation (1) is also solution of the boundary integral equation on S

$$\frac{1}{2}p(\mathbf{x}) = \int_S \left[p(\mathbf{y}) \frac{\partial G}{\partial n_y}(\mathbf{x},\mathbf{y}) - \frac{\partial p}{\partial n_y}(\mathbf{y}) G(\mathbf{x},\mathbf{y}) \right] d\mathbf{y} \tag{2}$$

with the Green's function

$$G(\mathbf{x},\mathbf{y}) = \frac{e^{ikr}}{4\pi r} \tag{3}$$

and $\mathbf{r} = |\mathbf{x} - \mathbf{y}|$. To avoid numerical problems in the formulation (2) for some frequencies associated to resonances of the interior acoustic domain, the Burton and Miller's formulation is used [2]. This formulation leads to singular kernels. For regularizing these

singularities, a variational formulation of the boundary integral equation is used, which finally leads to the following relation:

$$\begin{aligned}
\frac{1}{2}\int_S \tilde{p}(\mathbf{x})p(\mathbf{x})d\mathbf{x} + \frac{i}{2k}\int_S \tilde{p}(\mathbf{x})\frac{\partial p}{\partial n_x}(\mathbf{x})d\mathbf{x} = \\
\int_S\int_S \tilde{p}(\mathbf{x})p(\mathbf{y})\frac{\partial G}{\partial n_y}(\mathbf{x},\mathbf{y})d\mathbf{y}d\mathbf{x} - \int_S\int_S \tilde{p}(\mathbf{x})\frac{\partial p}{\partial n_y}(\mathbf{y})G(\mathbf{x},\mathbf{y})d\mathbf{y}d\mathbf{x} + \\
\frac{i}{k}\left\{\int_S\int_S k^2\tilde{p}(\mathbf{x})\mathbf{n}_x.\mathbf{n}_y G(\mathbf{x},\mathbf{y})p(\mathbf{y})d\mathbf{y}d\mathbf{x} - \int_S\int_S (\mathbf{n}_x\wedge\nabla_x\tilde{p}(\mathbf{x})).(\mathbf{n}_y\wedge\nabla_y p(\mathbf{y}))G(\mathbf{x},\mathbf{y})d\mathbf{x}d\mathbf{y}\right. \\
\left. - \int_S\int_S \tilde{p}(\mathbf{x})\frac{\partial p}{\partial n_y}(\mathbf{y})\frac{\partial G}{\partial n_x}(\mathbf{x},\mathbf{y})d\mathbf{y}d\mathbf{x}\right\} \qquad (4)
\end{aligned}$$

for all test functions $\tilde{p}$ on the boundary S.

However, the precedent formulation leads to full matrices and heavy computations. For improving the efficiency of such computations, the Fast Multiple Method (FMM) was introduced by Rokhlin in 1985 to solve boundary integral equations for the 2D Laplace equation in $O(N)$ operations [7]. Nowadays, the FMM is applied in multiple areas, such as fluid mechanics [10] or elastodynamics [3]. The development for acoustics was mainly initiated by Rokhlin [8].

Here, we use a multilevel FMM, based on a hierarchical space partition tree (oct-tree in 3D) and using the variational formulation (4). It is based on multipole developments of Green's kernels such as

$$G(\mathbf{x},\mathbf{y}) = \frac{ik}{4\pi}\sum_{n=1}^{L}(2n+1)\sum_{m=-n}^{n}\bar{I}_n^m(k,\mathbf{y},\mathbf{y}_c)O_n^m(k,\mathbf{x},\mathbf{y}_c) \qquad (5)$$

with $|\mathbf{y}-\mathbf{y}_c| < |\mathbf{x}-\mathbf{y}_c|$. In equation (5), one has:

$$\begin{cases} I_n^m(k,\mathbf{y},\mathbf{y}_c) = j_n(k\,|\mathbf{y}-\mathbf{y}_c|)Y_n^m\left(\frac{\mathbf{y}-\mathbf{y}_c}{|\mathbf{y}-\mathbf{y}_c|}\right) \\ O_n^m(k,\mathbf{x},\mathbf{y}_c) = h_n^{(1)}\left(k\,|\mathbf{x}-\mathbf{y}_c|\right)Y_n^m\left(\frac{\mathbf{x}-\mathbf{y}_c}{|\mathbf{x}-\mathbf{y}_c|}\right) \end{cases} \qquad (6)$$

with j_n, $h_n^{(1)}$ Bessel and Hankel functions of order n, Y_n^m the spherical harmonic of degree n and order m, defined by:

$$Y_n^m(\theta,\phi) = \sqrt{\frac{(n-m)!}{(n+m)!}}P_n^m(\cos\theta)e^{im\phi} \qquad (7)$$

with P_n^m the Legendre polynomial of degree n and order m. These developments are introduced in formulation (4), then usual relations for multipole expansion (ME), multipole to multipole (M2M), multipole to local (M2L), local to local (L2L) and local expansion (LE) are computed. See [5] for details on the FMM.

Another possibility, much faster but quite approximate, is to use the high frequency approximation on the surface S:

$$p \approx \rho c v_n \tag{8}$$

meaning that the surface impedance is supposed to be given by ρc. In this case, the acoustic power radiated by the surface is

$$P_a = \int_S \frac{1}{2} Re(p^* v_n) ds = \frac{\rho c}{2} \int_S |v_n|^2 ds = \rho c P_v \tag{9}$$

with P_a is the acoustic power and P_v is defined as a vibration energy.

These different formulations are used to compute the sound radiation for squeal noise, they are compared to find the most efficient for each case and finally a mixed formulation is proposed.

2 EXAMPLE OF SOUND RADIATION

2.1 Mesh of the structure

We study here three parts of the braking system which are the disc, the pads and the caliper, see figure 1.

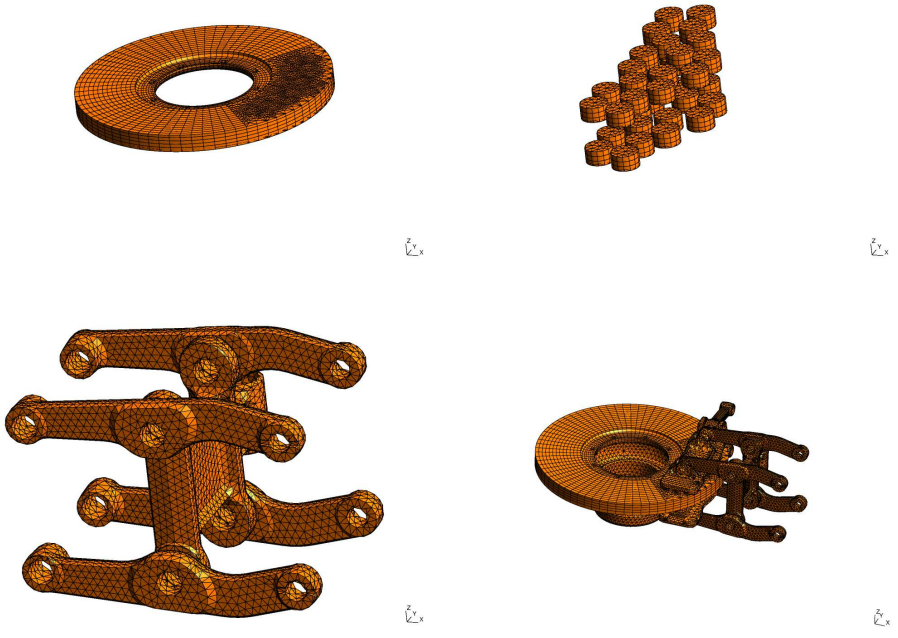

Figure 1: braking system with disc (upper left), pads (upper right), caliper (bottom left) and full brake (bottom right)

2.2 Surface velocities

The computation of surface velocities on the brake surface from the structural dynamic analysis leads to a large number of frequencies. An example of mean root square surface velocities of the disc for the complete spectrum is shown in figure 2. As it can be seen,

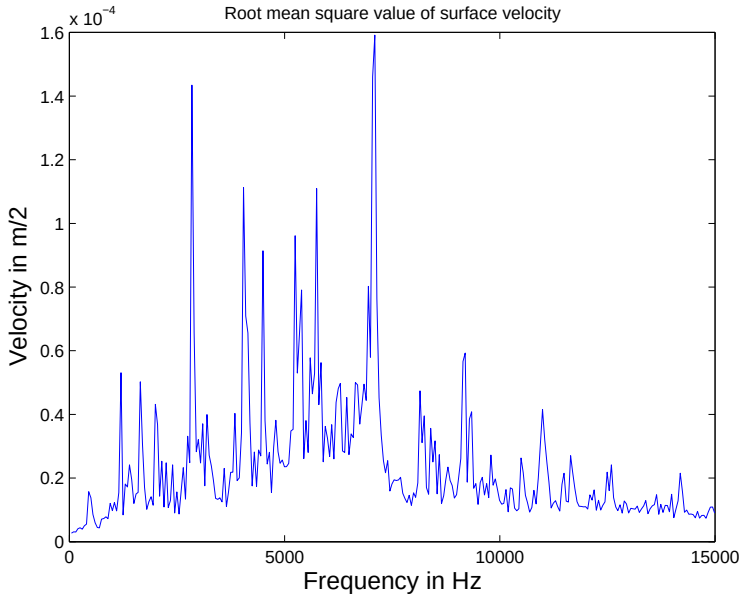

Figure 2: Root mean square velocity on the disc versus the frequency.

there are some clear spectral lines but also a broadband spectrum. An example of surface velocity on the disc for the frequencies 2848Hz and 7096Hz are given in figure 3. They exhibit complex patterns other the whole disc or other a small part only. To reduce the computations, the most energetic frequencies are selected. So, for each frequency f_i, the energy of vibration on the surface S is defined by $E_i = \int_S |v_i|^2 ds$. Defining the maximal error which is tolerated by the parameter ϵ and supposing the frequencies are ordered such that $E_1 \geq E_2 \geq ... \geq E_{n_{tot}}$, the n selected frequencies are such

$$\sum_{i=1}^{i=n} \int_S |v_i|^2 ds \geq (1-\epsilon) \sum_{i=1}^{i=n_{tot}} \int_S |v_i|^2 ds \tag{10}$$

Then the n frequencies are computed by the FMM and the $n_{tot} - n$ others are computed by the approximate method.

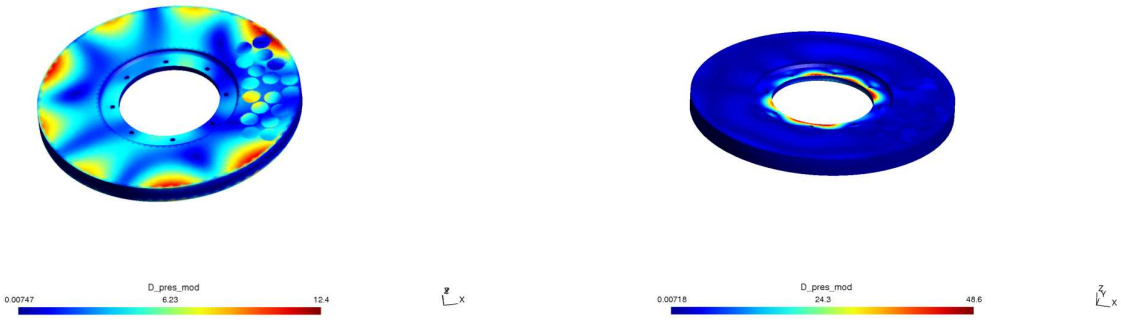

Figure 3: Normal velocities at the surface of the disc for the frequencies 2848Hz (left) and 7096Hz (right).

2.3 Radiated power

The acoustic power radiated by a structure is defined by

$$P = \frac{1}{2}\int_S Re(pv_n^*)ds \tag{11}$$

This quantity has been computed for the most energetic frequencies for the disc, the pads and the caliper. The frequencies computed by FMM are given in table 1.

Table 1: Computed frequencies in Hz for the different parts

Frequency	Disc	Caliper	Pads
f_1	2849	2749	2849
f_2	4048	2849	4048
f_3	5747	4048	5247
f_4	7046	4148	5747
f_5	7096	-	6947

The results are presented in figure 4 for the simplified method and for the FMM. As it can be seen, the radiated power is rather correctly approximated by the simplified method for these frequencies. The total power is obtained by summing the contributions of the different frequencies by the formula

$$P_{tot} = \Delta f \sum_{i=1}^{i=n} P_i \tag{12}$$

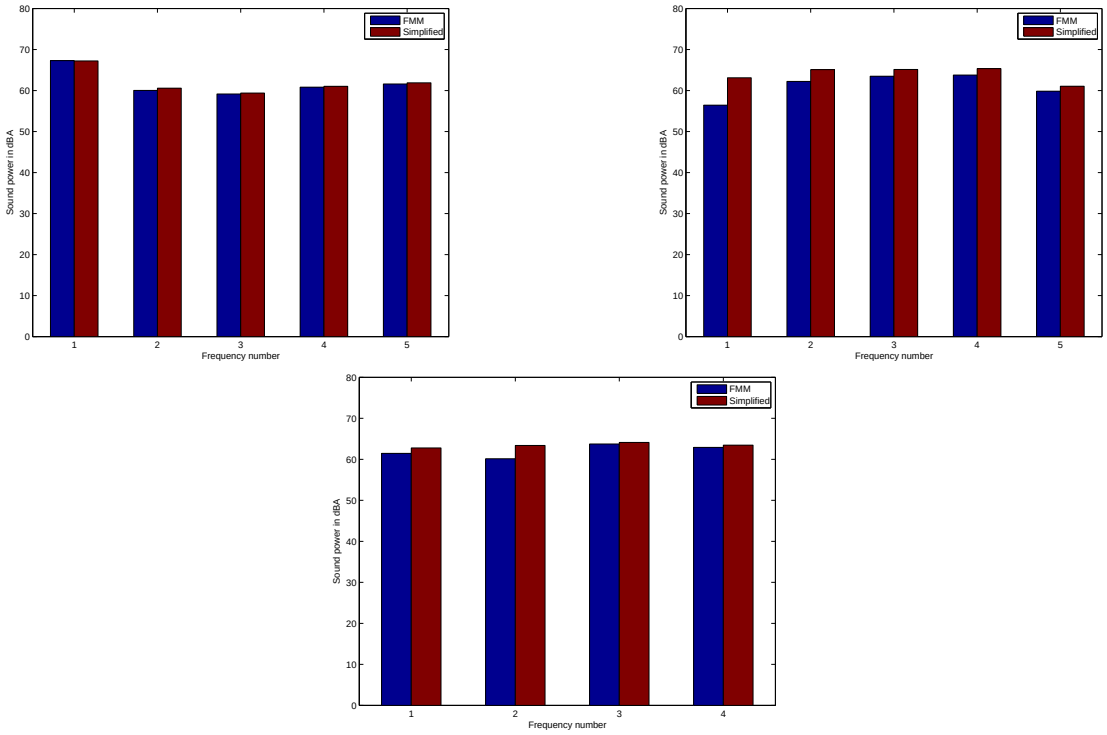

Figure 4: Sound power radiated by the disc (upper left), the pads (upper right) and the caliper (bottom)

where P_i is the power radiated by the frequency f_i and Δf is the frequency step. This computation is done for different values of ϵ using formula 10 to select the frequencies. Figure 5 presents the number of frequencies to keep versus the error in dB defined by $e = 10\log_{10}(1-\epsilon)$. It can be seen that if an error of 2dB on the total vibration energy

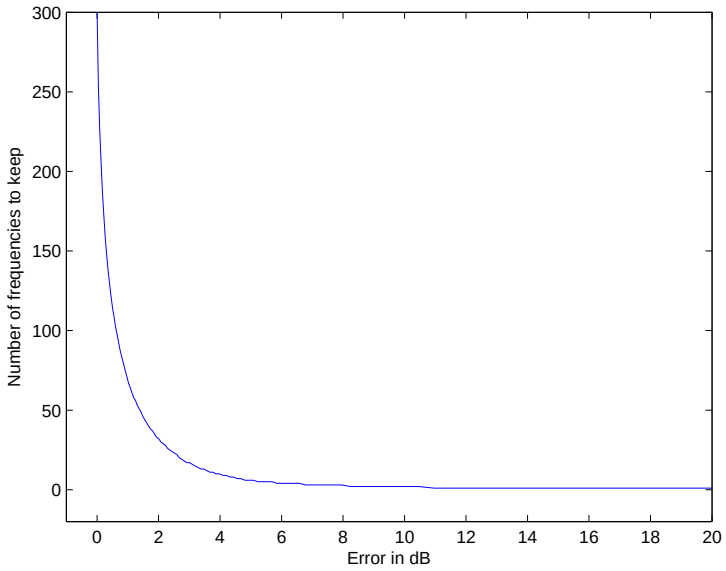

Figure 5: Number of frequencies to keep

is accepted, only about 30 frequencies need to be kept over a total of 300. The acoustic power in third octave bands is presented in figure 6 for the disc. One can see the wide band of this spectrum. The total power is 95dBA.

2.4 Pressure at points and directivity of the sound pressure

The sound level is obtained by

$$L = 20\log_{10}\frac{|p|}{2.10^{-5}} \tag{13}$$

and is computed for different points $p_1 = (1,0,0)$, $p_2 = (0,1,0)$ and $p_3 = (0,0,1)$. Results are presented in figure 7 for the disc and the caliper. For some points and frequencies, the difference between the FMM and the approximate method is larger than for the acoustic power.

The sound pressure has also been plotted in a rectangle $[-2m\ 2m] \times [0.3m\ 2.3m]$ above the disc in the xz plane. The results are plotted in figure 8. A rather strong directivity of the sound pressure can be seen.

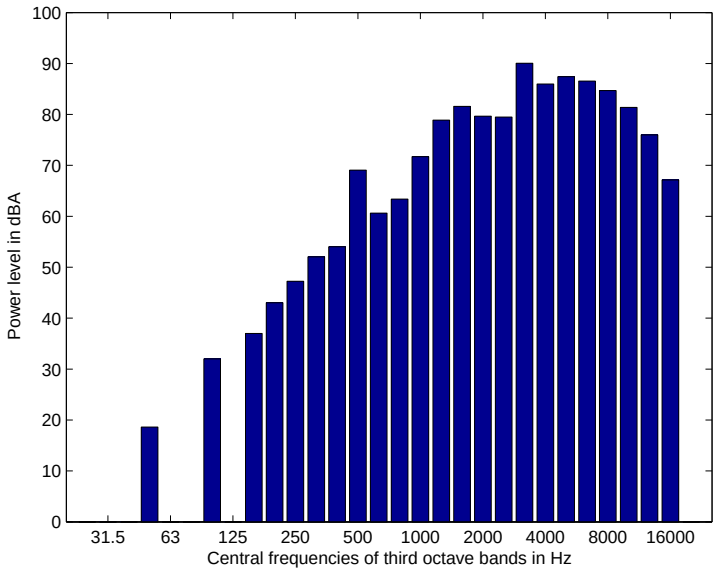

Figure 6: Power level in third octave.

3 CONCLUSION

The computation of acoustic radiation for high frequency squeal noise has been presented. Comparison of FMM and approximate method leads to the proposition of a mixed approach where the dominant frequencies are computed by FMM while the other frequencies are computed by an approximate method. This seems especially useful for the computation of the radiated acoustic power.

ACKNOWLEDGMENT

The author gratefully acknowledge ADEME (Agence De l'Environnement et de la Matrise de l'Energie) who has funded this research through the project Acoufren.

REFERENCES

[1] D. Brizard, O. Chiello, J.-J. Sinou, and X. Lorang. Performances of some reduced bases for the stability analysis of a disc/pads system in sliding contact. *J. of Sound and Vib.*, 330(4):703–720, 2011.

[2] A. J. Burton and G. F. Miller. The application of integral equation methods to the numerical solution of some exterior boundary-value problems. *Proceedings of the Royal Society of London*, 323:201–220, 1971.

[3] S. Chaillat. *Méthode multipôle rapide pour les équations intégrales de frontière en élastodynamique 3-D. Application à la propagation d'ondes sismiques.* Thèse de doctorat, Ecole Nationale des Ponts et Chaussées, 2008.

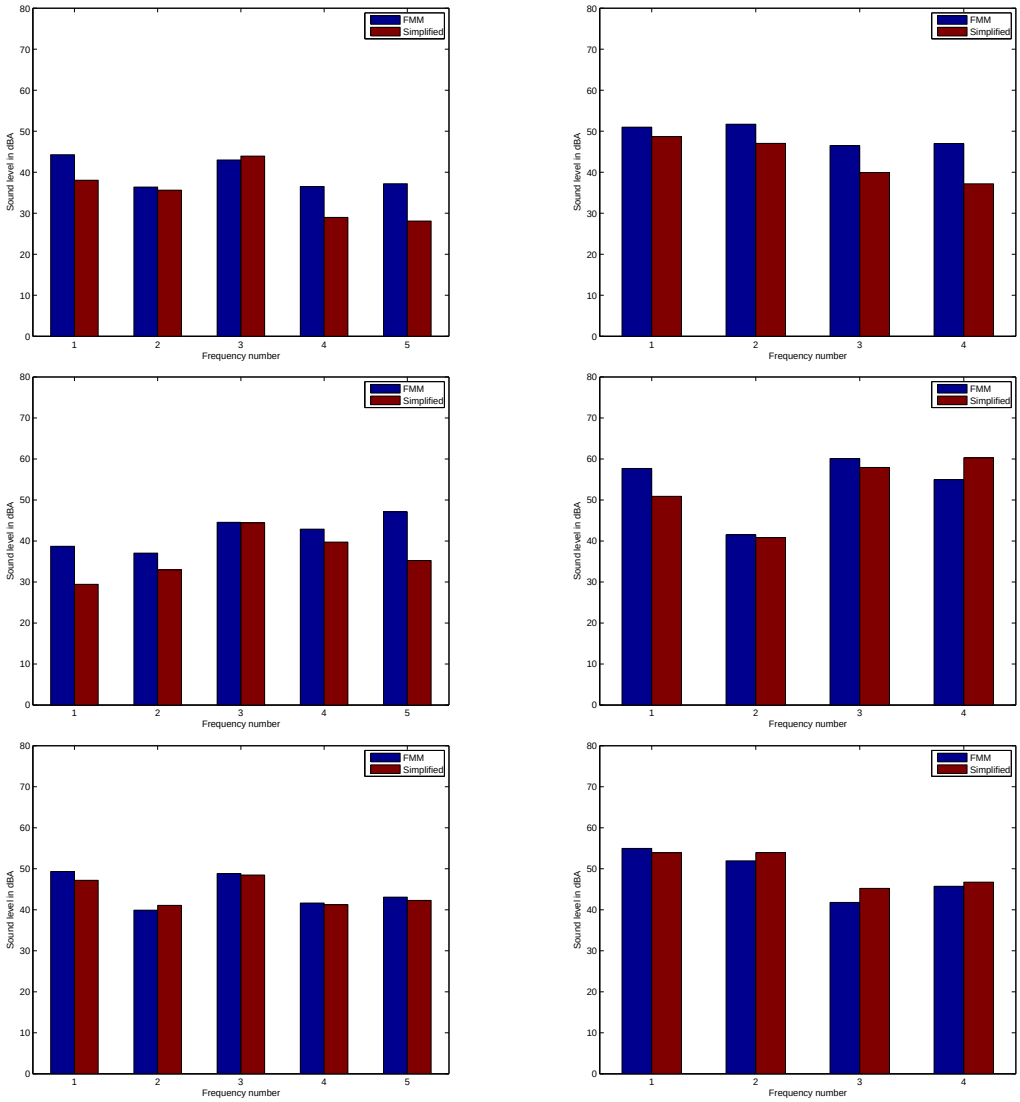

Figure 7: Sound level at point 1 (upper figure), point 2 (middle figure) and point 3 (bottom figure) for the disc (left figures) and the caliper (right figures)

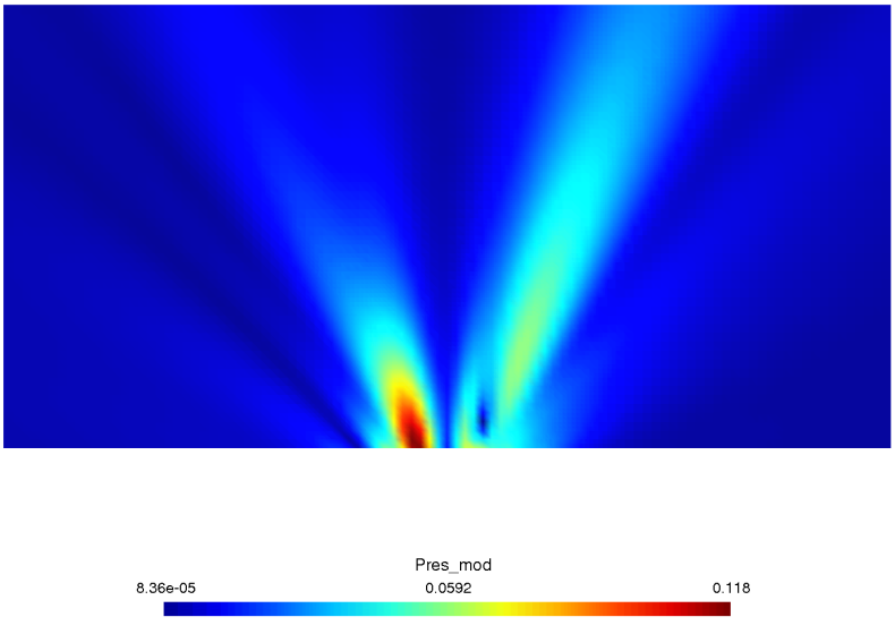

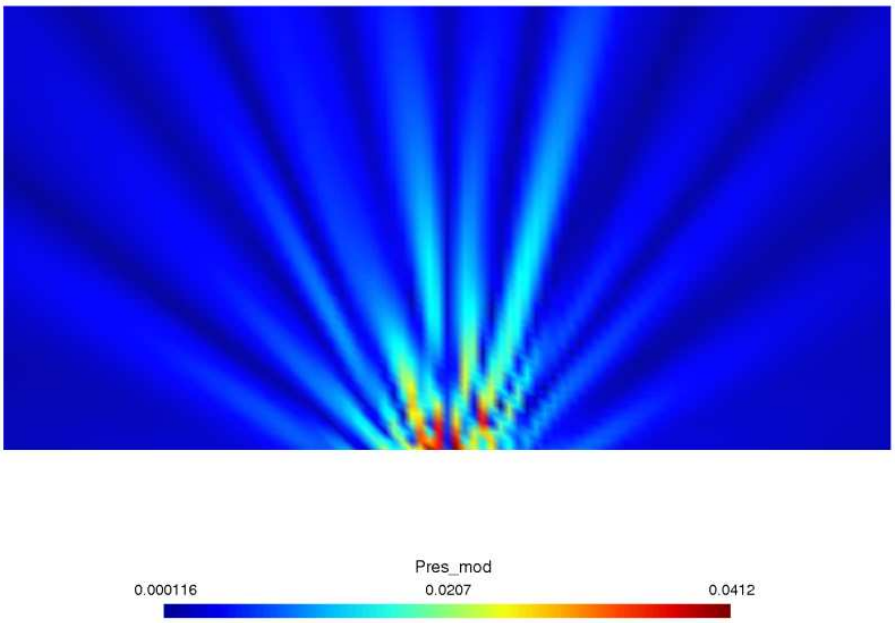

Figure 8: Directivity of the sound pressure in the xz plane for the frequency 2848Hz (upper figure) and 7096Hz (lower figure)

[4] O. Chiello and X. Lorang. Numerical investigations into the squeal propensity of a railway disc brake. *J. of Acous. Soc. of America*, 123(5):3171, 2008.

[5] Y. Liu. *Fast Multipole Boundary Element Method - Theory and Applications in Engineering*. Cambridge - University Press, 2009.

[6] X. Lorang. *Instabilité des structures en contact frottant : Application au crissement des freins disque de TGV*. Thèse de doctorat, Ecole Polytechnique, 2007.

[7] V. Rokhlin. Rapid solution of integral equations of classical potential theory. *J. Comput. Phys.*, 60:187–207, 1985.

[8] V. Rokhlin. Rapid solution of integral equation of scattering theory in two dimensions. *J. Comput. Phys.*, 86:414–439, 1990.

[9] J.-J. Sinou, A. Loyer, O. Chiello, G. Mogenier, X. Lorang, F. Cocheteux, and S. Bellaj. A global strategy based on experiments and simulations for squeal prediction on industrial railway brakes. *J. of Sound and Vib.*, 332(20):5068–5085, 2013.

[10] R. Yokota and L. A. Barba. Comparing the treecode with fmm on gpus for vortex particle simulations of a leapfrogging vortex ring. *Computers & Fluids*, 45(1):155 – 161, 2011.